



CrossMark  
click for updates

Cite this: *Lab Chip*, 2016, 16, 199

## LabDisk with complete reagent prestorage for sample-to-answer nucleic acid based detection of respiratory pathogens verified with influenza A H3N2 virus†

F. Stumpf,<sup>‡\*a</sup> F. Schwemmer,<sup>‡b</sup> T. Hutzenlaub,<sup>a</sup> D. Baumann,<sup>a</sup> O. Strohmeier,<sup>a</sup> G. Dingemanns,<sup>c</sup> G. Simons,<sup>c</sup> C. Sager,<sup>d</sup> L. Plobner,<sup>e</sup> F. von Stetten,<sup>ab</sup> R. Zengerle<sup>abf</sup> and D. Mark<sup>a</sup>

Portable point-of-care devices for pathogen detection require easy, minimal and user-friendly handling steps and need to have the same diagnostic performance compared to centralized laboratories. In this work we present a fully automated sample-to-answer detection of influenza A H3N2 virus in a centrifugal LabDisk with complete prestorage of reagents. Thus, the initial supply of the sample remains the only manual handling step. The self-contained LabDisk automates by centrifugal microfluidics all necessary process chains for PCR-based pathogen detection: pathogen lysis, magnetic bead based nucleic acid extraction, aliquoting of the eluate into 8 reaction cavities, and real-time reverse transcription polymerase chain reaction (RT-PCR). Prestored reagents comprise air dried specific primers and fluorescence probes, lyophilized RT-PCR mastermix and stick-packaged liquid reagents for nucleic acid extraction. Employing two different release frequencies for the stick-packaged liquid reagents enables on-demand release of highly wetting extraction buffers, such as sequential release of lysis and binding buffer. Microfluidic process-flow was successful in 54 out of 55 tested LabDisks. We demonstrate successful detection of the respiratory pathogen influenza A H3N2 virus in a total of 18 LabDisks with sample concentrations down to  $2.39 \times 10^4$  viral RNA copies per ml, which is in the range of clinical relevance. Furthermore, we detected RNA bacteriophage MS2 acting as internal control in 3 LabDisks with a sample concentration down to 75 plaque forming units (pfu) per ml. All experiments were applied in a 2 kg portable, laptop controlled point-of-care device. The turnaround time of the complete analysis from sample-to-answer was less than 3.5 hours.

Received 24th July 2015,  
Accepted 12th November 2015

DOI: 10.1039/c5lc00871a

www.rsc.org/loc

## Introduction

Respiratory tract infections were the fourth most common cause of death in 2012 according to the WHO, accounting for roughly 3.1 million deaths worldwide.<sup>1</sup> Currently, nucleic acid detection is generally performed in central laboratories.

However, analysis in centralized laboratories typically leads to turnaround times in the order of days. Due to the lack of these fast diagnostics, empirical antibiotic therapy is the common practice. Antibiotics are often used on suspicion with no effect on the course of the disease.<sup>2</sup> Such unnecessary use of antibiotics is one of the leading reasons for the spread of multi-resistant pathogens, which have evolved to become a major threat to global public health.<sup>3</sup>

Therefore there is an urgent need for a diagnostic system which is able to rapidly test for infections at the point-of-care.<sup>4</sup> An ideal point-of-care system would be rapid, easy to use by non-experts with minimal hands on time and able to detect multiple pathogenic species in parallel in a small light-weight device. While a range of sample-to-answer systems for nucleic acid based detection of respiratory infections are commercially available, no system satisfies all the needs of such a point-of-care system (see Table 1). Most of the sample-to-answer systems listed in Table 1 are not suitable for point-of-care usage by non-experts due to their CLIA moderate

<sup>a</sup> Hahn-Schickard, Georges-Koehler-Allee 103, 79110 Freiburg, Germany.

E-mail: Fabian.Stumpf@Hahn-Schickard.de

<sup>b</sup> Laboratory for MEMS Applications, IMTEK - Department of Microsystems Engineering, University of Freiburg, Georges-Koehler-Allee 103, 79110 Freiburg, Germany

<sup>c</sup> PathoFinder B.V., Randwycksingel 45, 6229 EG Maastricht, The Netherlands

<sup>d</sup> Medical Care Center, Dr. Stein and colleagues, Wallstraße 10, 41061 Moenchengladbach, Germany

<sup>e</sup> Agrobiogen GmbH Biotechnologie, Larezhäuser 2-3, 86567 Hilgertshausen, Germany

<sup>f</sup> BIOS – Centre for Biological Signalling Studies, University of Freiburg, 79110 Freiburg, Germany

† Electronic supplementary information (ESI) available: Details of respiratory qPCR panels and rotational frequency protocol. See DOI: 10.1039/c5lc00871a

‡ These authors contributed equally to this work.



**Table 1** Commercially available and the LabDisk system for detection of respiratory pathogens

Company	Number of processing devices	Size and weight of devices	Degree of multiplexing	Complexity	Time-to-result
Alere Inc., Alere™ i	1	14 × 15 × 21 cm <sup>3</sup> , 3 kg	2-plex	CLIA waived	15 min
Cepheid Inc., GeneXpert® I	1 <sup>a</sup>	10 × 29 × 30 cm <sup>3</sup> , 4 kg	5-plex	CLIA moderate complexity	<120 min
Roche Molecular Systems Inc., cobas® LiaT	1	11 × 19 × 24 cm <sup>3</sup> , 3.76 kg	2-plex	CLIA moderate complexity	25–60 min
Focus Diagnostics Inc., 3M™ Integrated Cyclor	1 <sup>a</sup> + barcode reader	21 × 31 × 31 cm <sup>3</sup> , 8 kg	3-plex	CLIA moderate complexity	~60 min
BioFire Diagnostics Inc., FilmArray®	2 <sup>a</sup> + barcode reader	17 × 25 × 39 cm <sup>3</sup> , 9 kg 4 × 11 × 18 <sup>b</sup> cm <sup>3</sup> , 0.45 <sup>b</sup> kg	20-plex	CLIA moderate complexity	60 min
Hahn-Schickard, LabDisk	1 <sup>a</sup>	15 × 18 × 28 cm <sup>3</sup> , 2 kg	1-plex <sup>c</sup>	1 manual step (not CLIA certified)	210 <sup>d</sup> min

<sup>a</sup> Laptop/desktop-PC needed for instrument control and data analysis. <sup>b</sup> Size and weight of second device of the FilmArray® system (loading station). <sup>c</sup> 1-plex per reaction cavity and geometric-multiplexing<sup>7</sup> demonstrated, due to 8 reaction cavities potential for 8 × 4-plex = 32-plex in future developments. <sup>d</sup> Reduction of time-to-result was not object of this publication.

complexity. The Alere™ i system (Alere Inc., USA) is the only CLIA waived product though it still requires multiple manual handling steps (e.g. manual washing of swabs). The Alere™ i system provides a fast time-to-result due to its isothermal amplification but is therefore limited in degree of multiplexing (two geometrical separated single-plex reactions). In fact, all systems are significantly limited in their degree of multiplexing ( $\leq 5$ -plex), with the exception of the FilmArray® system (BioFire Diagnostics, Inc., USA) which consists of 2 devices (loading station and FilmArray® instrument) and just as the 3M™ Integrated Cyclor (Focus Diagnostics Inc., USA) system, doesn't provide prestorage of liquid reagents.<sup>5,6</sup>

The lack of liquid reagent prestorage results in additional handling steps which require additional hands-on time and training to use the system correctly. Thus, there is no point-of-care system offering truly minimal handling, while featuring a high degree of multiplexing as well as prestorage of all required liquid reagents. Lab-on-a-Chip devices are a promising candidate for point-of-care systems to detect nucleic acids. Different platforms with varying automation principles have been suggested for this task.<sup>8–11</sup> Centrifugal microfluidics is especially suitable, due to its simple interfaces and the fact that it only requires a single actuator.<sup>12–15</sup> Process chains demonstrated in centrifugal microfluidics are lysis,<sup>16–18</sup> nucleic acid extraction<sup>19–25</sup> and real-time amplification of nucleic acids.<sup>7,26–33</sup> Due to recent advances in magnetic bead handling,<sup>24</sup> valving,<sup>34–40</sup> aliquoting<sup>41–43</sup> and pumping<sup>44–47</sup> integration of full sample-to-answer systems on the centrifugal microfluidic LabDisk platform now became feasible. Kim *et al.* presented an integrated centrifugal microfluidic disk for detection of food-borne pathogens. Valving was realized *via* laser actuated ferrowax valves. The laser diode used for actuation of valves was also used for thermal lysis and amplification *via* RPA. After RPA the amplification product is diluted and read-out is performed on a lateral flow strip.<sup>48</sup> Jung *et al.* presented a Lab-on-a-Disk for detection of H1N1 from purified viral RNA or viral lysates. RNA was

extracted *via* sequential flow of liquids over stationary microbeads.<sup>21</sup> After extraction, the eluate was amplified *via* reverse transcription-LAMP. The chip did not include multiplexing or lysis.<sup>49</sup> Roy *et al.* presented a centrifugal microfluidic disk for detection of *Bacillus atrophaeus* subsp. *globigii* spores. The disk includes mechanical cellular lysis, PCR amplification, digestion of amplicons and hybridization to a microarray. The disk is fabricated in thermoplastic elastomer, which allowed for sealing of the PCR chamber during PCR amplification by external pressure.<sup>50</sup> G. Czilwik *et al.* presented a centrifugal microfluidic disk for neonatal sepsis. The disk extracts DNA from blood serum using a bind-wash-elute protocol automated using silica coated magnetic beads transported between adjacent chambers. The eluate is used to rehydrate a lyophilized polymerase pellet for pre-amplification of the target DNA. The pre-amplified target DNA is then pumped radially inwards by centrifugo-dynamic inward pumping and aliquoted into 13 reaction cavities for individual real-time PCR of the pathogens of interest. Detection of a sepsis panel has been demonstrated with four different bacterial pathogens.<sup>51</sup>

So far, no centrifugal microfluidic disk for nucleic acid sample-to-answer analysis with complete prestorage of reagents has been demonstrated. For the first time we demonstrate a fully automated sample-to-answer system – comprising prestorage of all required reagents – for detection of respiratory pathogens based on centrifugal microfluidics. The disk includes RNA extraction *via* chemical lysis and a bind-wash-elute protocol, based on transport of silica coated magnetic particles between adjacent chambers. The eluate is pumped to the aliquoting structure *via* centrifugo-dynamic inward pumping.<sup>52</sup> The eluate is aliquoted into 8 × 10 μl aliquots, potentially allowing for 32-plex multiplexing (geometrical 8-plex distribution with up to 4-plex detection per reaction cavity using 4 different detection channels for real-time RT-PCR) with subsequent RT-PCR of the extracted RNA. All required reagents are prestored, either as dried reagents (magnetic beads, primer and fluorescence probes, lyophilized RT-PCR mastermix) or as liquid reagents using miniature



stick-packs. Supply of the sample into the LabDisk remains the only manual handling step. The LabDisk is processed in a LabDisk player, a 15 cm × 18 cm × 28 cm small and 2 kg light device suitable for operation at the point-of-care. Functionality of the system was verified with an influenza real-time PCR assay using the respiratory pathogen influenza A H3N2 virus.

## Materials and methods

### LabDisk fabrication

All microfluidic structures were designed as 3D-CAD drawing (SolidWorks, Dassault Systèmes SolidWorks Corp., France) and manufactured in-house by Hahn-Schickard Lab-on-a-Chip Design and Foundry Service ([www.hahn-schickard.de/en/manufacturing/lab-on-a-chip-design-foundry-service](http://www.hahn-schickard.de/en/manufacturing/lab-on-a-chip-design-foundry-service)) applying microthermoforming by soft lithography ( $\mu$ TSL)<sup>7</sup> as rapid prototyping and scalable replication process.<sup>53</sup> In brief, the microstructures were milled in a 4 mm thick polymethylmethacrylate (PMMA) substrate using an ultra-precision milling machine (Kern EVO, KERN Microtechnik GmbH, Germany). The PMMA substrate is cast with polydimethylsiloxane (PDMS) (Elastosil RT-607, Wacker Chemie AG, Germany) and cured at 80 °C for 2 hours before the PDMS master mold with the elevated microfluidic structures is post-cured at 200 °C for one hour in order to prevent outgassing of remaining monomers of the PDMS during the following thermoforming process. The cured PDMS master mold is placed into a hot embossing machine (HEX01, Jenoptik AG, Germany) for micro-thermoforming of the LabDisk (diameter = 130 mm) using 188  $\mu$ m thick cyclic olefin polymer foil (COP, ZF14, TOPAS Advanced Polymers GmbH, Germany). COP acts as an appropriate fabrication material for LabDisk production<sup>7</sup> due to its beneficial properties like mechanical and thermal stability, high transparency as well as biological inertness. Sample inlet and air vent were cut into the LabDisk using a CO<sub>2</sub> laser (PLS 3.60, Universal Laser Systems, Inc., USA). The surfaces of the nucleic acid extraction chambers which later come in contact with extraction buffers and magnetic beads during bead transfer as well as the stick-pack chambers were hydrophobically coated by pipetting 120  $\mu$ L of a 0.5% w/w Teflon AF solution (E. I. du Pont de Nemours and Company, USA) dissolved in Fluorinert FC-77 (3M Co., USA). Used surface coating does not have inhibiting effects on the assay performance.

### Reagent prestorage

Liquid buffers for nucleic acid extraction (Agrobiogen GmbH, Germany) are pre-stored in miniature stick-packs<sup>54</sup> – 30 mm × 9 mm aluminum pouches allowing long-term storage and featuring frangible seals, which are opened due to liquid pressure under centrifugation at a very well defined spinning frequency. For liquid reagent prestorage, mass production of miniature stick-packs was applied on a commercial stick-packaging machine (SBL50, Merz-Verpackungsmaschinen GmbH, Germany) with a cycle time of 1.4 seconds per stick-

pack. Modification of sealing parameters during stick-pack fabrication enables rotational frequency protocol defined on-demand release of 200  $\mu$ L highly wetting binding buffer at the target release frequency of 70 Hz after the lysis procedure. All other liquid buffers (180  $\mu$ L lysis buffer, 200  $\mu$ L washing buffer 1, 200  $\mu$ L washing buffer 2 and 120  $\mu$ L elution buffer) are previously released at the target release frequency of 50 Hz. Oligonucleotide solutions – for multiplex detection of 22 pathogens (18 viruses and 4 atypical bacteria) which are generally recognized to cause a serious respiratory infection (RealAccurate Quadruplex Respiratory qPCR panels, PathoFinder B.V., The Netherlands; see ESI† Table S1 for detailed panel information) – consisting of primers and fluorescence probes were mixed with trehalose (Carl Roth GmbH & Co. KG, Germany) as stabilizing agent,<sup>55</sup> pipetted into the reaction cavities of the LabDisk (for detailed allocation of the panels see Fig. 1 & 3) resulting in a 23-plex (18 viruses, 4 atypical bacteria and an internal control) detection by geometrical 8-plex distribution with up to 4-plex detection per reaction cavity using 4 different detection channels (FAM, Yakima Yellow, Texas Red and TYE665) for real-time RT-PCR. Subsequently magnetic beads (Agrobiogen GmbH, Germany) – including an excess of magnetic beads to prevent nucleic acid overloading – were mixed with trehalose and pipetted into the lysis chamber. Oligonucleotide solutions and magnetic beads were air dried for 4 hours at room temperature and ambient pressure (final trehalose concentration: 200 mM for magnetic beads, 56 mM for primer and fluorescence probes). Our previously reported protocol confirmed long-term functionality of air-dried oligonucleotide primers and fluorescent hydrolysis probes stabilized by trehalose for 1 year.<sup>55</sup> After loading of stick-packs into the corresponding chambers, each of the reaction cavities was loaded with one bead of lyophilized polymerase (One-Step RT-PCR Master Lyophilisate, Jena Bioscience GmbH, Germany). These lyophilisates provide the RT-PCR mastermix after being dissolved by the RNA eluate and contain according to manufacturer SCRIPT Reverse Transcriptase, Hot Start Polymerase, dNTPs, reaction buffer, MgCl<sub>2</sub> and stabilizers. After loading and drying of reagents the LabDisk was sealed with an adhesive foil (Polyolefin-foil #900320, HJ-Bioanalytik GmbH, Germany). A 0.2  $\mu$ m pore size PTFE membrane filter (Merck Millipore KGaA, Germany) is attached to cover the air vent in order to prevent contamination by aerosols. Fixation and positioning holes were cut into the LabDisk using a CO<sub>2</sub> laser (PLS 3.60, Universal Laser Systems, Inc., USA).

### Processing device

Processing of the LabDisk was conducted in a prototype LabDisk player (Qiagen Lake Constance GmbH, Germany) featuring PCR-thermocycling, four channel real-time fluorescence detection and the possibility to run predefined rotational frequency protocols consisting of a sequence of rotational frequencies (0–90 Hz), accelerations, decelerations (from 0.1 Hz s<sup>-1</sup> through to 50 Hz s<sup>-1</sup>) and temperature variations (for 10  $\mu$ L liquid: heating ramp 0.7 K s<sup>-1</sup> and cooling



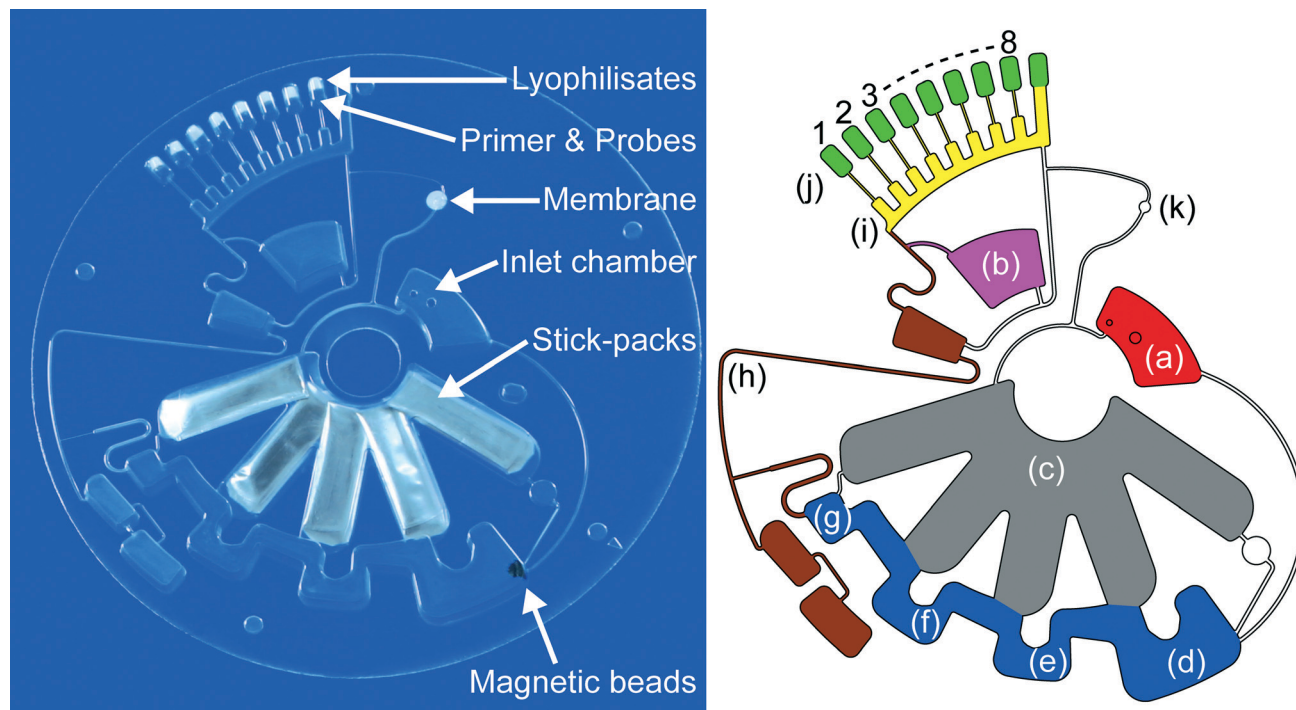


**Fig. 1** Photograph (left) of the LabDisk for sample-to-answer nucleic acid based detection of respiratory pathogens with complete reagent prestorage and a CAD drawing (right) of the microfluidic structure. The sample is supplied into the inlet chamber (a) while liquid reagents are prestored in stick-packs and placed therein into the overlapping stick-pack chambers (c) which are connected to the Teflon coated nucleic acid extraction structure (d–g) consisting of the lysis and binding chamber (d) wherein the magnetic beads are prestored, the washing chamber 1 (e) and 2 (f) and the eluate chamber (g). The microfluidic channels and pneumatic chambers in the area of (h) are used for inward pumping of the eluate into the aliquoting structure (i) and transferred subsequently to the reaction cavities (j). Primers and fluorescence probes are prestored in the reaction cavities as well as the RT-PCR lyophilisates. For optional reagent addition during the development phase of the LabDisk, chamber (b) was implemented. It can be used e.g. for loading a liquid RT-PCR mastermix instead of lyophilisates. The air vent (k) is covered by a hydrophobic membrane prohibiting contamination by aerosol dissemination.

ramp  $1.0 \text{ K s}^{-1}$ ). For fluorescence detection of the reaction cavities as well as magnetic bead transfer a precise positioning accuracy of  $0.1^\circ$  is provided. The LabDisk is mounted on an aluminum holder fixed to the rotational axis inside the processing chamber providing stationary magnets (#S-08-04-N and #S-06-03-N, Webcraft GmbH Supermagnete.de, Germany) on two radial positions for automated transfer of magnetic beads during nucleic acid extraction process.<sup>24</sup> Temperature control of the processing chamber is realized by heating of circulating air with heating wires and valve-regulated influx of ambient air is used for cooling. Due to the size and weight of the portable processing device ( $15 \text{ cm} \times 18 \text{ cm} \times 28 \text{ cm}$ ; 2 kg) the LabDisk player is suitable for operation at the point-of-care.

### Microfluidic layout

The LabDisk for sample-to-answer nucleic acid based detection of respiratory pathogens consists of an inlet chamber for the sample which is connected to the lysis and binding chamber of the nucleic acid extraction structure. Stick-packs are pre-stored in chambers of 3.55 mm height. To save space, the chambers overlap at inner radii. Appropriate stick-pack chambers are connected to different chambers of the DNA

extraction structure, the lysis and binding chamber, containing the prestored magnetic beads, followed by the washing chamber 1, the washing chamber 2 and the elution chamber. All these radially outward arranged chambers are interconnected by radially inwards placed bridging areas for the transfer of the magnetic beads. The elution chamber is connected to a fluidic network consisting of channels and pneumatic chambers<sup>52</sup> for eluate transfer to the aliquoting structure, a sloping feed channel with branched off metering chambers which are connected to the cross contamination free<sup>7</sup> reaction cavities *via* centrifugo-pneumatic valves.<sup>41</sup> Prestored primer, fluorescence probes and RT-PCR mastermix lyophilisates will be rehydrated as soon as the reaction mix is transferred to the reaction cavities. The microfluidic layout of the LabDisk is shown in Fig. 1.

### Fluidic processing and RT-PCR based amplification

The LabDisk is mounted onto the holder in the LabDisk player and after supplying  $200 \mu\text{l}$  of the sample into the inlet chamber, the automated microfluidic process flow (Fig. 2) begins by starting the rotational frequency protocol (see ESI† Table S2 for detailed protocol). Centrifugal forces are used for microfluidic unit operations like transport, mixing,



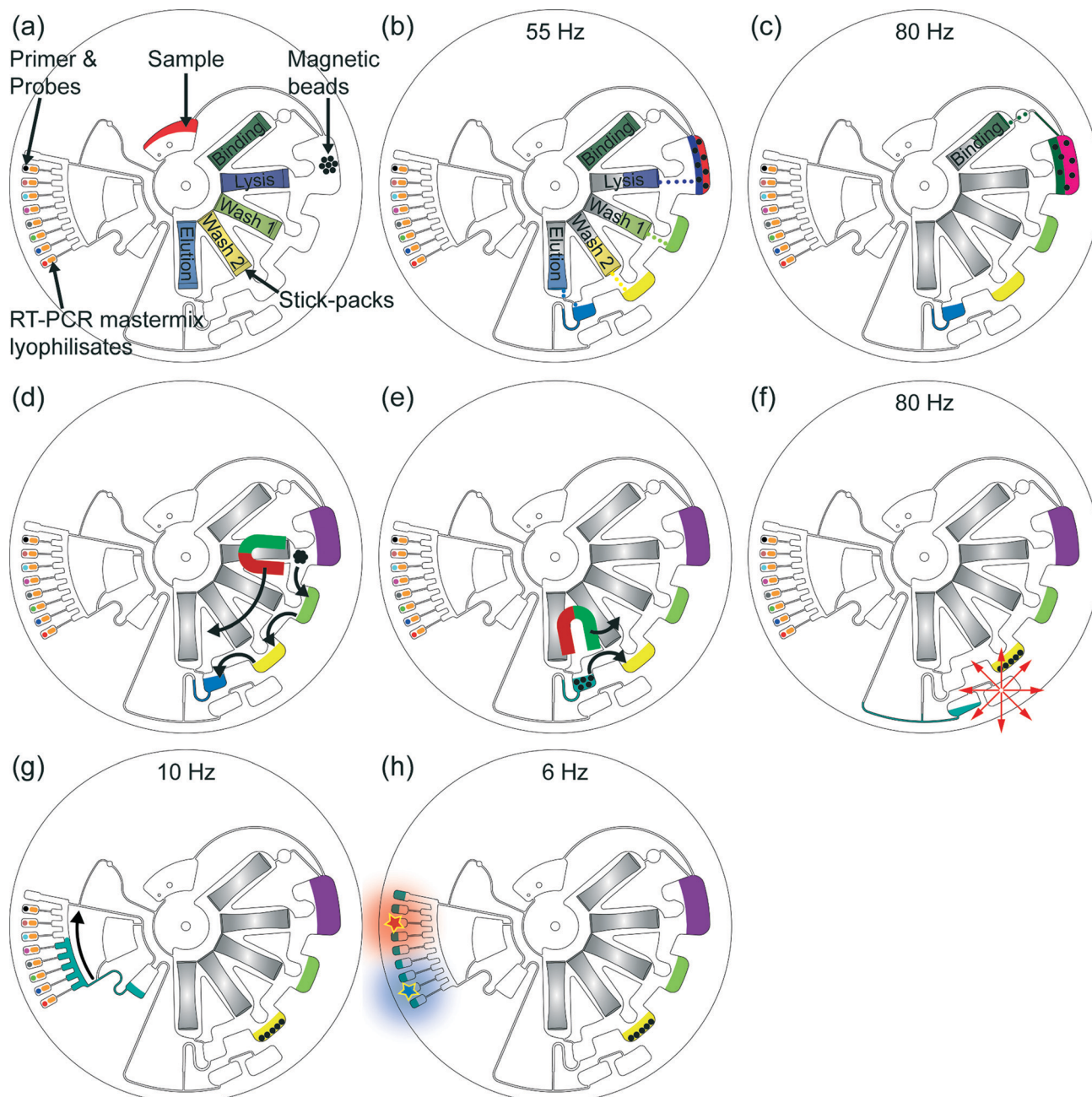


**Fig. 2** Centrifugal microfluidic process-flow: (a) the 200  $\mu\text{l}$  sample is supplied into the LabDisk. Then, the automated rotational frequency protocol starts: the sample is pumped radially outwards into the lysis chamber by centrifugation and therein prestored magnetic beads get rehydrated. (b) At a frequency of 55 Hz the RNA extraction buffers (except the binding buffer) are released out of the stick-packs and transferred to the corresponding and adjacent chambers of the RNA extraction structure, magnetic beads get rehydrated and resuspended and sample lysis starts while applying shake mode mixing (frequency alteration between 2 Hz and 14 Hz). The chemical lysis was applied for 10 minutes. All application times during extraction procedure were applied as specified by the manufacturer of the reagents. (c) The binding buffer is added to the lysed sample at a frequency of 80 Hz enabling RNA binding to the magnetic beads. The binding step takes 5 minutes and is accompanied by shake mode mixing. (d) Magnetic beads are transferred through the washing buffers by magnetic actuation.<sup>24</sup> In each washing buffer the magnetic beads were mixed for 3 minutes by magnet induced collection of the magnetic beads (0 Hz for 3 seconds) followed by resuspension due to acceleration to the frequency of 10 Hz (hold for 7 seconds). Finally, the magnetic beads are transferred into the elution buffer and the RNA is released of the beads in the following 5 minutes. (e) After RNA elution the magnetic beads are transferred into the previous washing chamber, preventing potential failures in the following microfluidic procedure induced by the magnetic beads. (f) The RNA eluate is transferred to the radially inward placed collection chamber by centrifugo-dynamic inward pumping.<sup>52</sup> (g) By applying 10 Hz the RNA eluate is transferred into the aliquoting structure, preparing 10  $\mu\text{l}$  aliquots. The excess volume of RNA eluate is collected in the adjacent waste reservoir located at the end of the aliquoting structure. At 20 Hz aliquots of 10  $\mu\text{l}$  are centrifuged into each of the eight reaction cavities inducing rehydration of the therein prestored RT-PCR lyophilisates as well as of primers and fluorescent probes. (h) Finally, reverse transcription and PCR with real-time fluorescent readout are performed.



valving and aliquoting. As initial sample material we used the RNA bacteriophage MS2 (DSM-13767, type: *Levivirus*, species: *Enterobacteria* phage MS2, DSMZ GmbH, Germany) acting as internal control of the used respiratory panels and was diluted with SM buffer, pH 7.5 (Alfa Aesar GmbH & Co KG, Germany) and applied with the concentration of  $75 \text{ pfu ml}^{-1}$ . As respiratory pathogen sample we used the influenza A virus (H3N2) (ATCC® VR822™, classification: *Orthomyxoviridae*, influenza virus A; strain: A/Victoria/3/75, American Type Culture Collection (ATCC), USA) with a stock concentration of  $2.39 \times 10^6$  viral RNA copies per ml (determined by digital PCR) which was diluted with  $1 \times$  Tris-EDTA buffer (Sigma-Aldrich Co. LLC., USA) to a 1:10 and a 1:100 dilution. After RNA extraction the eluate is transferred into the reaction cavities where the eluate rehydrates the prestored RT-PCR lyophilisates as well as the primer and fluorescence probes. Subsequently the RT-PCR with real-time fluorescent signal readout is performed.

## Results and discussion

### Microfluidic performance

The microfluidic process flow as illustrated in Fig. 2 was successfully demonstrated in 54 out of 55 LabDisks. In one experiment the eluate was not forwarded to the aliquoting structure due to a clogged channel of the air vent system. As there was no eluate transfer into the reaction cavities, false negative results were prevented.

### Liquid reagent release

Stick-pack reagent release frequency was optically determined using a stroboscopic image acquisition system (Biofluidix GmbH, Germany) with a total of 100 stick-packs (20 stick-packs per extraction buffer). For evaluation frequency was increased with an acceleration rate of  $0.1 \text{ Hz s}^{-1}$  and the results are stated in Table 2.

The measured release frequencies demonstrate successful performance of on-demand frequency controlled reagent release. For ensuring the controlled reagent release in the LabDisk the parameters in the rotational frequency protocol were set to 60 seconds at 55 Hz for the lysis, washing 1, washing 2 and elution buffer release and 60 seconds at 80 Hz for the binding buffer release.

Assuming a normal distribution of release frequencies, we can estimate the error rates for the different stick-packs based on Table 2. The system will fail, if a) the stick-pack containing the binding buffer opens prematurely (release frequency  $\leq 55 \text{ Hz}$ , 12.9 sigma) or not at all (release frequency  $> 80 \text{ Hz}$ , 7.9 sigma), b) the stick-pack containing the lysis buffer does not open at the initial 55 Hz rotation (4.7 sigma) or c) one of the other stick-packs does not open at the binding buffer release frequency of 80 Hz ( $> 35$  sigma). Based on the cumulated error rates for individual stick-packs, the error rate for full disks is 1 out of 825.000.

### Preliminary detection of internal control of respiratory panels

For initial experiments and demonstration of geometrical multiplexing capability the RNA bacteriophage MS2 – acting as the internal control (IC) of the respiratory panels – was used as sample. Due to the composition of the respiratory panels (see ESI† Table S1 for detailed panel information) the IC oligonucleotides was absent in two of the reaction cavities (detailed oligonucleotide solution allocation in Fig. 1 & 3) and thus no positive fluorescence signals were expected in these cavities. For this experiment we initially equipped chamber (b) (see Fig. 1) with  $100 \mu\text{l}$  qScript One-Step RT-qPCR buffer (Quanta BioSciences, Inc., USA) instead of using the RT-PCR mastermix lyophilisates. The RT-PCR buffer is transferred to the reaction cavities ( $10 \mu\text{l}$  each) during microfluidic process steps (a) and (b), illustrated in Fig. 2. After supplying of  $200 \mu\text{l}$  RNA bacteriophage MS2 ( $75 \text{ pfu ml}^{-1}$ ) into the LabDisks the automated microfluidic processing (illustrated in Fig. 2) was started. The usage of the liquid RT-PCR buffer results in a final reaction volume of  $20 \mu\text{l}$  in the reaction cavities. The subsequent real-time RT-PCR begins with the initial RT step ( $50 \text{ }^\circ\text{C}$  for 10 minutes) followed by initial denaturation at  $95 \text{ }^\circ\text{C}$  for 1 minute and 45 thermocycles ( $95 \text{ }^\circ\text{C}$  for 20 seconds;  $60 \text{ }^\circ\text{C}$  for 60 seconds) with real-time fluorescent signal readout. A total of three LabDisks were successfully processed and an exemplary result of one of the experiments is shown in Fig. 3. Positive amplification signals were detected by real-time RT-PCR in all six reaction cavities containing the IC oligonucleotide solution and, respectively, no amplification was detected in the two reaction cavities where IC oligonucleotide solution was absent, demonstrating sample-to-answer detection and geometrical multiplexing as success of the experiments. The time to result was less than 3 hours.

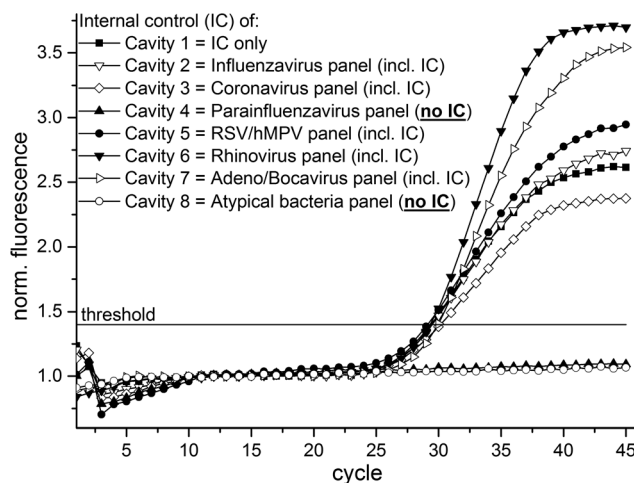


Fig. 3 Fluorescence signal for parallel RT-PCR reactions acquired after the annealing step in each reaction cavity. Except reaction cavity 4 (parainfluenza panel) and reaction cavity 8 (atypical bacteria panel) each reaction cavity contained primers and fluorescence probe also detecting RNA bacteriophage MS2 as internal control. Missing primer and fluorescence probes for internal control led to the negative signal in these two reaction cavities.



**Table 2** Extraction buffer release frequencies of 100 stick-packs (20 per extraction buffer) show successful performance enabling on-demand frequency controlled reagent release

	Binding buffer	Lysis buffer	Washing buffer 1	Washing buffer 2	Elution buffer
Prestored volume [ $\mu\text{m}$ ]	200	180	200	200	200
Mean release frequency [Hz], $n = 20$	70.5	51.7	49.8	49.7	48.8
Standard deviation [Hz]	1.2	0.7	1.0	0.8	0.8
CV [%]	1.7	1.4	2.0	1.6	1.6

### Detection of influenza H3N2 virus

For demonstration of the fully automated sample-to-answer process with sample supply as the only manual handling step and detection of a respiratory pathogen we used influenza A virus (H3N2) (ATCC® VR822™) (American Type Culture Collection (ATCC), USA) as sample in a total of 18 LabDisks with prestorage of all reagents. Three virus concentrations were used as sample and the concentration of the stock solution was determined by digital PCR being  $2.39 \times 10^6$  viral RNA copies per ml. Additionally the 1:10 dilution (concentration approx.:  $2.39 \times 10^5$  viral RNA copies per ml) and the 1:100 dilution (concentration approx.:  $2.39 \times 10^4$  viral RNA copies per ml) from stock were used as sample. The final reaction volume was 10  $\mu\text{l}$  in each reaction cavity. The real-time RT-PCR begins with the initial RT step (50 °C for 30 minutes) followed by initial denaturation at 95 °C for 5 minutes and 45 thermocycles consisting of denaturation (94 °C for 5 seconds) as well as annealing and elongation steps (55 °C for 40 seconds) with real-time fluorescence signal readout. The fluorescence signals of all 18 experiments were identically normalized and plotted in Fig. 4. We achieved positive amplification signals in 18 out of 18 LabDisks especially emphasizing the positive amplification results in the 5 LabDisks with the 1:100 dilution as sample (concentration approx.:  $2.39 \times 10^4$  viral RNA copies per ml). Literature describes the range of clinical relevance of pathogen detection for the influenza A

virus in between of  $10^5$  viral RNA copies per ml<sup>56</sup> and  $10^6$  viral RNA copies per ml.<sup>57</sup> We detected the influenza A H3N2 virus with approximately fourfold lower concentration than clinical relevance and thus obtaining sufficient sensitivity for clinical relevance. The time-to-result was less than 3.5 hours. Clinical real patient samples like sputum are typically of varying physical properties like viscosity and homogeneity. Therefore, an integrated sample preparation unit for liquefaction and homogenization of clinical real patient samples will be implemented and evaluated onto the LabDisk in future projects.

### Conclusion and outlook

The fully automated sample-to-answer process including chemical lysis, RNA extraction and subsequent real-time RT-PCR was demonstrated in the centrifugal LabDisk platform. Reduction to one initial manual handling step (sample supply) was realized by prestorage of all required liquid and solid reagents. The use of frequency dependent on-demand release of liquid buffers out of stick-packs facilitates handling and post-lysis addition of highly wetting binding buffer. Verification was performed with RNA bacteriophage MS2 as sample (75 pfu per ml) and additionally the influenza A H3N2 virus was detected with clinical relevant sensitivity. The space-saving microfluidic design leaves room for an improved LabDisk design containing more reaction cavities enabling the implementation of more pathogen panels and thus increases the degree of multiplexity. By further compression of the presented microfluidic design two identical structures could be implemented on one LabDisk. Furthermore the internal control might be prestored by air drying into the sample chamber preventing manual addition of the internal control to the sample.

The next step is a clinical validation of all integrated pathogen panels which either requires off- or on-disk homogenization and liquefaction of crude clinical samples.<sup>58</sup> Handling of viscous and inhomogeneous crude clinical samples, such as sputum or tracheal and bronchial secretion is a challenging task which is not solved in any of the discussed commercially available systems (Table 1). Handling of inhomogeneous sample material may be addressed in further developments by adding a defined inlet port with an integrated sample preparation unit onto the LabDisk. In addition we will significantly reduce the time-to-result in further developments by shortening of the nucleic extraction protocol and reverse transcription process time or the usage of time-saving

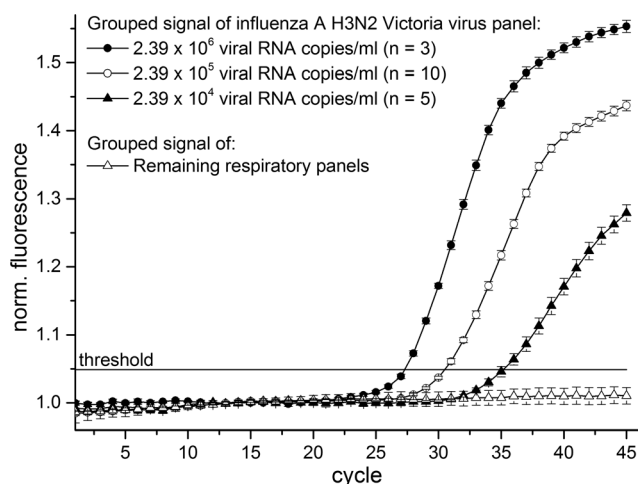


**Fig. 4** Combined fluorescence signals of 18 individual LabDisk experiments with different influenza A H3N2 virus concentrations as sample.



isothermal amplification methods *e.g.* recombinase polymerase amplification (RPA) or loop mediated isothermal amplification (LAMP). Geometrical multiplexing<sup>41</sup> guarantees high degree of multiplexing even by applying isothermal amplification methods. Furthermore, the aliquoting structure in the current disk could be replaced with centrifugal step emulsification,<sup>59</sup> which would allow for fully integrated sample-to-digital-answer disposables.

Overall, the LabDisk features 1) a disposable with only one structured part and a flat sealing foil, 2) a simple reader with a rotational motor, heating unit and fluorescent detector, and 3) the possibility to use standard PCR assays without microarrays. This could be very attractive features when commercializing the system.

## Acknowledgements

The authors like to thank for financial support from the EU FP7-HEALTH program (research project PARCIVAL – “Partner Network for a Clinically Validated Multi-Analyte Lab-on-a-Chip Platform”, grant agreement No. GA 278090).

## Notes and references

- World Health Organisation, <http://www.who.int/mediacentre/factsheets/fs310/en/> (accessed 07-22-2015, 2015).
- C. C. Butler, K. Hood, T. Verheij, P. Little, H. Melbye, J. Nuttall, M. J. Kelly, S. Mölstad, M. Godycki-Cwirko, J. Almirall, A. Torres, D. Gillespie, U. Rautakorpi, S. Coenen and H. Goossens, *BMJ*, 2009, **338**, b2242.
- World Health Organisation, *Antimicrobial resistance: global report on surveillance*, World Health Organization, 2014.
- The White House National Action Plan for Combating Antibiotic-Resistant Bacteria*, 2015, [https://www.whitehouse.gov/sites/default/files/docs/national\\_action\\_plan\\_for\\_combating\\_antibiotic-resistant\\_bacteria.pdf](https://www.whitehouse.gov/sites/default/files/docs/national_action_plan_for_combating_antibiotic-resistant_bacteria.pdf) (accessed 07-22-2015, 2015).
- K. H. Rand, H. Rampersaud and H. J. Houck, *J. Clin. Microbiol.*, 2011, **49**, 2449–2453.
- M. Xu, X. Qin, M. L. Astion, J. C. Rutledge, J. Simpson, K. R. Jerome, J. A. Englund, D. M. Zerr, R. T. Migita, S. Rich, J. C. Childs, A. Cent and M. A. Del Beccaro, *Am. J. Clin. Pathol.*, 2013, **139**, 118–123.
- M. Focke, F. Stumpf, B. Faltin, P. Reith, D. Bamarni, S. Wadle, C. Müller, H. Reinecke, J. Schrenzel, P. Francois, D. Mark, G. Roth, R. Zengerle and F. von Stetten, *Lab Chip*, 2010, **10**, 2519–2526.
- R. H. Liu, J. Yang, R. Lenigk, J. Bonanno and P. Grodzinski, *Anal. Chem.*, 2004, **76**, 1824–1831.
- J. Pipper, M. Inoue, L. F.-P. Ng, P. Neuzil, Y. Zhang and L. Novak, *Nat. Med.*, 2007, **13**, 1259–1263.
- S. Schumacher, J. Nestler, T. Otto, M. Wegener, E. Ehrentreich-Förster, D. Michel, K. Wunderlich, S. Palzer, K. Sohn, A. Weber, M. Burgard, A. Grzesiak, A. Teichert, A. Brandenburg, B. Koger, J. Albers, E. Nebling and F. F. Bier, *Lab Chip*, 2012, **12**, 464–473.
- G. Xu, T.-M. Hsieh, D. Y. S. Lee, E. M. Ali, H. Xie, X. L. Looi, E. S.-C. Koay, M.-H. Li and J. Y. Ying, *Lab Chip*, 2010, **10**, 3103–3111.
- D. Mark, S. Haeberle, G. Roth, F. von Stetten and R. Zengerle, *Chem. Soc. Rev.*, 2010, **39**, 1153–1182.
- O. Strohmeier, M. Keller, F. Schwemmer, S. Zehnle, D. Mark, F. von Stetten, R. Zengerle and N. Paust, *Chem. Soc. Rev.*, 2015, **44**, 6187–6229.
- J. Ducrée, S. Haeberle, S. Lutz, S. Pausch, F. von Stetten and R. Zengerle, *J. Micromech. Microeng.*, 2007, **17**, S103–S115.
- L. X. Kong, A. Perebikovskiy, J. Moebius, L. Kulinsky and M. Madou, *J. Lab. Autom.*, 2015, DOI: 10.1177/2211068215588456.
- H. Kido, M. Micic, D. Smith, J. Zoval, J. Norton and M. Madou, *Colloids Surf., B*, 2007, **58**, 44–51.
- J. Kim, S. Hee Jang, G. Jia, J. V. Zoval, N. A. Da Silva and M. J. Madou, *Lab Chip*, 2004, **4**, 516–522.
- J. Siegrist, R. Gorkin, M. Bastien, G. Stewart, R. Peytavi, H. Kido, M. Bergeron and M. Madou, *Lab Chip*, 2010, **10**, 363–371.
- Y.-K. Cho, J.-G. Lee, J.-M. Park, B.-S. Lee, Y. Lee and C. Ko, *Lab Chip*, 2007, **7**, 565–573.
- J. Hoffmann, D. Mark, S. Lutz, R. Zengerle and F. von Stetten, *Lab Chip*, 2010, **10**, 1480–1484.
- J. H. Jung, B. H. Park, Y. K. Choi and T. Seo, *Lab Chip*, 2013, **13**, 3383–3388.
- A. Kloke, A. R. Fiebach, S. Zhang, L. Drechsel, S. Niekrawietz, M. M. Hoehl, R. Kneusel, K. Panthel, J. Steigert, F. von Stetten, R. Zengerle and N. Paust, *Lab Chip*, 2014, **14**, 1527–1537.
- B. H. Park, J. H. Jung, H. Zhang, N. Y. Lee and T. S. Seo, *Lab Chip*, 2012, **12**, 3875–3881.
- O. Strohmeier, A. Emperle, G. Roth, D. Mark, R. Zengerle and F. von Stetten, *Lab Chip*, 2013, **13**, 146–155.
- O. Strohmeier, S. Keil, B. Kanat, P. Patel, M. Niedrig, M. Weidmann, F. Hufert, J. Drexler, R. Zengerle and F. von Stetten, *RSC Adv.*, 2015, **5**, 32144–32150.
- M. Amasia, M. Cozzens and M. J. Madou, *Sens. Actuators, B*, 2012, **161**, 1191–1197.
- P.-A. Auroux, Y. Koc, A. deMello, A. Manz and P. J. R. Day, *Lab Chip*, 2004, **4**, 534–546.
- M. Focke, F. Stumpf, G. Roth, R. Zengerle and F. von Stetten, *Lab Chip*, 2010, **10**, 3210–3212.
- J. H. Jung, S. J. Choi, B. H. Park, Y. K. Choi and T. S. Seo, *Lab Chip*, 2012, **12**, 1598–1600.
- S. Lutz, P. Weber, M. Focke, B. Faltin, J. Hoffmann, C. Müller, D. Mark, G. Roth, P. Munday, N. Armes, O. Piepenburg, R. Zengerle and F. von Stetten, *Lab Chip*, 2010, **10**, 887–893.
- O. Strohmeier, S. Laßmann, B. Riedel, D. Mark, G. Roth, M. Werner, R. Zengerle and F. von Stetten, *Microchim. Acta*, 2014, **181**, 1681–1688.
- O. Strohmeier, N. Marquart, D. Mark, G. Roth, R. Zengerle and F. von Stetten, *Anal. Methods*, 2014, **6**, 2038–2046.
- M. M. Hoehl, M. Weißert, A. Dannenberg, T. Nesch, N. Paust, F. Stetten, R. Zengerle, A. H. Slocum and J. Steigert, *Biomed. Microdevices*, 2014, **16**, 375–385.





- 34 M. M. Aeinehvand, F. Ibrahim, S. W. Harun, W. Al-Faqheri, T. H. G. Thio, A. Kazemzadeh and M. Madou, *Lab Chip*, 2014, **14**, 988–997.
- 35 W. Al-Faqheri, F. Ibrahim, T. H. G. Thio, J. Moebius, K. Joseph, H. Arof and M. Madou, *PLoS One*, 2013, **8**, e58523.
- 36 R. Gorkin III, C. E. Nwankire, J. Gaughran, X. Zhang, G. G. Donohoe, M. Rook, R. O'Kennedy and J. Ducee, *Lab Chip*, 2012, **12**, 2894–2902.
- 37 D. J. Kinahan, S. M. Kearney, N. Dimov, M. T. Glynn and J. Ducee, *Lab Chip*, 2014, **14**, 2249–2258.
- 38 B. S. Lee, Y. U. Lee, H.-S. Kim, T.-H. Kim, J. Park, J.-G. Lee, J. Kim, H. Kim, W. G. Lee and Y.-K. Cho, *Lab Chip*, 2011, **11**, 70–78.
- 39 Y. Ouyang, S. Wang, J. Li, P. S. Riehl, M. Begley and J. P. Landers, *Lab Chip*, 2013, **13**, 1762–1771.
- 40 F. Schwemmer, S. Zehnle, D. Mark, F. von Stetten, R. Zengerle and N. Paust, *Lab Chip*, 2015, **15**, 1545–1553.
- 41 D. Mark, P. Weber, S. Lutz, M. Focke, R. Zengerle and F. von Stetten, *Microfluid. Nanofluid.*, 2011, **10**, 1279–1288.
- 42 P. Andersson, G. Jesson, G. Kylberg, G. Ekstrand and G. Thorsén, *Anal. Chem.*, 2007, **79**, 4022–4030.
- 43 F. Schwemmer, T. Hutzenlaub, D. Buselmeier, N. Paust, F. von Stetten, D. Mark, R. Zengerle and D. Kosse, *Lab Chip*, 2015, **15**, 3250–3258.
- 44 K. Abi-Samra, L. Clime, L. Kong, R. Gorkin III, T.-H. Kim, Y.-K. Cho and M. Madou, *Microfluid. Nanofluid.*, 2011, **11**, 643–652.
- 45 N. Godino, R. Gorkin III, A. V. Linares, R. Burger and J. Ducee, *Lab Chip*, 2013, **13**, 685–694.
- 46 R. Gorkin, L. Clime, M. Madou and H. Kido, *Microfluid. Nanofluid.*, 2010, **9**, 541–549.
- 47 M. C. R. Kong and E. D. Salin, *Anal. Chem.*, 2010, **82**, 8039–8041.
- 48 T.-H. Kim, J. Park, C.-J. Kim and Y.-K. Cho, *Anal. Chem.*, 2014, **86**, 3841–3848.
- 49 J. H. Jung, B. H. Park, S. J. Oh, G. Choi and T. S. Seo, *Biosens. Bioelectron.*, 2015, **68**, 218–224.
- 50 E. Roy, G. Stewart, M. Mounier, L. Malic, R. Peytavi, L. Clime, M. Madou, M. Bossinot, M. G. Bergeron and T. Veres, *Lab Chip*, 2015, **15**, 406–416.
- 51 G. Czilwik, T. Messinger, O. Strohmeier, S. Wadle, F. von Stetten, N. Paust, G. Roth, R. Zengerle, P. Saarinen, J. Niittymäki, K. McAllister, O. Sheils and D. Mark, *Lab Chip*, 2015, **15**, 3749–3759.
- 52 S. Zehnle, F. Schwemmer, G. Roth, F. von Stetten, R. Zengerle and N. Paust, *Lab Chip*, 2012, **12**, 5142–5145.
- 53 M. Focke, D. Kosse, D. Al-Bamerni, S. Lutz, C. Müller, H. Reinecke, R. Zengerle and F. von Stetten, *J. Micromech. Microeng.*, 2011, **21**, 115002.
- 54 T. van Oordt, Y. Barb, J. Smetana, R. Zengerle and F. von Stetten, *Lab Chip*, 2013, **13**, 2888–2892.
- 55 M. Rombach, D. Kosse, B. Faltin, S. Wadle, G. Roth, R. Zengerle and F. von Stetten, *BioTechniques*, 2014, **57**, 151–155.
- 56 R. R. Jansen, J. Wieringa, S. M. Koekkoek, C. E. Visser, D. Pajkrt, R. Molenkamp, M. D. de Jong and J. Schinkel, *J. Clin. Microbiol.*, 2011, **49**, 2631–2636.
- 57 A. Franz, O. Adams, R. Willems, L. Bonzel, N. Neuhausen, S. Schweizer-Krantz, J. U. Rugeberg, R. Willers, B. Henrich, H. Schroten and T. Tenenbaum, *J. Clin. Virol.*, 2010, **48**, 239–245.
- 58 P.-H. Huang, L. Ren, N. Nama, S. Li, P. Li, X. Yao, R. A. Cuento, C.-H. Wei, Y. Chen, Y. Xie, A. A. Nawaz, Y. G. Alevy, M. J. Holtzman, J. P. McCoy, S. J. Levine and T. J. Huang, *Lab Chip*, 2015, **15**, 3125–3131.
- 59 F. Schuler, F. Schwemmer, M. Trotter, S. Wadle, R. Zengerle, F. von Stetten and N. Paust, *Lab Chip*, 2015, **15**, 2759–2766.

